

Effect of g -factor anisotropy in the magnetoresponse of organic light-emitting diodes at high magnetic fields

Daniel Nikiforov,^{1,2} Bagrat Khachatryan,^{1,2} Jenya Tilchin,^{2,3} Efrat Lifshitz,^{2,3} Nir Tessler,⁴ and Eitan Ehrenfreund^{1,2,*}

¹Physics Department, Technion-Israel Institute of Technology, Haifa 32000, Israel

²Solid State Institute, Technion-Israel Institute of Technology, Haifa 32000, Israel

³Shulich Chemistry Department, Technion-Israel Institute of Technology, Haifa 32000, Israel

⁴Department of Electrical Engineering, Technion-Israel Institute of Technology, Haifa 32000, Israel



(Received 2 July 2018; revised manuscript received 13 September 2018; published 17 December 2018)

We report the magnetic field and temperature dependences of magnetoconductance (MC) and magnetoelectroluminescence (MEL) in organic light emitting diodes (OLED) made of homopolymer organic layers. We show that in these OLEDs a spin mixing mechanism due to the anisotropy of the organic layer g factor has a significant effect in the measured $MC(B)$ and $MEL(B)$ at fields of order of ~ 1 T. We discuss the model of spin mixing among polaron pairs due to the anisotropy of the g factor and show that it can be described as an angle dependent Δg mechanism that is known to have significant magnetoresponse effects. We show that the internal structure of the polaron pair is material dependent rationalizing thus the differences in their electrical mobility.

DOI: [10.1103/PhysRevB.98.235204](https://doi.org/10.1103/PhysRevB.98.235204)

I. INTRODUCTION

Coherent superposition of spin states in bound pairs of polarons (spin $S = 1/2$) or triplet excitons (TE, $S = 1$) has been shown to be responsible for magnetic field effects in organic light emitting diodes (OLEDs) and other organic devices [1–3]. For example, the magnetoelectroluminescence (MEL) in an OLED based on MEH-poly(phenylene vinylene) (MEH-PPV) in both weak field ($B < 1$ mT) and low field ($B < 40$ mT) regimes [4] was accounted for in detail by the spin correlated polaron pair (PP) model that is based on the spin coherent evolution of the polaron-nuclear spin states [3–6]. Another example is the magnetic field dependence of delayed fluorescence caused by the fusion of a pair of TEs in organic substances; here the spin states of the triplet-triplet (TT) pair are maintained through the fusion giving rise to delayed fluorescence from the singlet state of the pair [1,6,7]. The loss of spin coherence limits the range of magnetic fields in which magnetic field effects (MFE) can be observed experimentally; the longer the coherence time, the smaller the magnetic field in which significant MFE can be observed. For the observed MEL response of width $\Delta B \sim 5$ mT, which is caused by the hyperfine polaron-proton interaction [3], it is required that the coherence time $\tau_{\text{coh}} > \hbar/(g\mu_B\Delta B) \sim 0.3$ ns in order to be observed.

Polaron pairs and TT pairs can be generated both by opposite charge carrier injection and through optical excitation in a nonthermal equilibrium state. They both provide a nonradiative recombination route that limits the OLED efficiency. Loss of spin coherence by pair decay (with decay time τ_d) is an ultimate process terminating all MFE. Another important characteristic time is the spin lattice relaxation time τ_{SL} , which quantifies the approach of the spin system toward

thermal equilibrium. For example, $\tau_{\text{SL}} = 80$ ns for polarons in regioregular poly(3-hexylthiophene) (P3HT) at $T = 300$ K [8], while τ_d is in the μ s range for polaron pairs.

We divide the mechanisms responsible for the MFE into two groups. The first group includes spin mixing by the hyperfine (HF) interaction [2,3], spin-orbit coupling (SOC) [9], and mechanisms that involve TE or TT pairs [1,6,10,11]. All these mechanisms can commonly be characterized by finite zero field splitting (ZFS) of the spin energy levels at $B = 0$ with spin content of each level that varies with the applied field. For these mechanisms the $MFE(B)$ response is limited to magnetic fields, B , smaller or of the order of $B_{\text{ZFS}} = \xi\mu_B^{-1}$, where ξ is the characteristic strength of the relevant spin mixing mechanism; beyond this field the effect eventually saturates [3,6]. The spin decay time scale for the mechanisms of this category is determined by B_{ZFS} ; the decay time should be longer than $\hbar\xi^{-1}$. The second group includes mechanisms, which in addition to the ZFS, the rate of spin mixing is field dependent in fields $B \gg B_{\text{ZFS}}$. A known mechanism in this group is the so-called “ Δg mechanism” in which the constituents of the pair have slightly different g factors. In the Δg mechanism in PP, the $S_z = 0$ (zero spin component along the field direction) levels of the spin $1/2$ pair are Zeeman split providing a faster $S \leftrightarrow T_0$ spin mixing mechanism at higher fields [12]. The MFE response is limited now not by B_{ZFS} but by $B_{\text{ZFS}}(\Delta g)^{-1}$ in the case of long decay time τ_d or by $\hbar(\mu_B\Delta g\tau_d)^{-1}$ in the case of very short τ_d [12,13]. As an example for this mechanism we mention charge transfer excitons (CTEs) with sub-ns decay time, τ_d , that are indirectly photoexcited in bulk heterostructure photovoltaic cells made of donor acceptor blends of regioregular P3HT (rrP3HT) and phenyl-C61-butyric acid methyl ester (PCBM), with $\Delta g \approx 0.002$; these CTEs showed very broad (width $\Delta B > 8$ T) magnetophotoconductance (MPC) response [12]. Another mechanism that may be attributed to the second group is “thermal spin polarization”, which is caused by thermal population of spin sublevels. This mechanism is more

*Author to whom correspondence should be addressed: eitane@technion.ac.il

effective at low temperatures and high magnetic fields as long as the species decay time is not much shorter than τ_{SL} , the characteristic time it takes to reach thermal equilibrium [13,14].

It is important to note that having spin dependent pair dissociation and/or recombination rates is critical for all of the above mechanisms; spin dependent decay was verified experimentally for a number of π -conjugated polymers [15,16].

A mechanism that was not discussed in detail previously is caused by the anisotropy of the g matrix. In low symmetry organic semiconductors (OS), such as P3HT and PPV derivatives, the g factor of the electron (hole) generated either by injection or photoexcitation is found experimentally to be anisotropic [17,18]. Electron paramagnetic resonance (EPR) studies at 95 GHz of photoinduced charges in poly(2-methoxy-5-(3-,7-dimethyloctyloxy)-1,4-phenylenevinylene) (MDMO-PPV)/PCBM blends showed two separate resonances at which the g factor differs by $\delta g \sim 10^{-3}$ [18]. Poly(2-methoxy-5-(2-ethylhexyloxy)-1,4-phenylenevinylene) (MEH-PPV) electrically detected magnetic resonance (EDMR) at 100–300 GHz also showed that the g matrix is anisotropic [19], whereas in poly(3,4-ethylenedioxythiophene):poly(styrene-sulfonate) (PEDOT:PSS) $\delta g \sim 10^{-4} - 10^{-3}$ [20]. For P3HT, EPR studies at 275 GHz revealed three resonances separated by $\delta g \sim 10^{-3} - 3 \times 10^{-3}$ [17]. When the g matrix is anisotropic the Zeeman split energy levels and their spin character depend not only on the magnitude of B , but also on its direction with respect to the anisotropy axes. In a given field direction the Zeeman Hamiltonian for a spin S is given by $H = g_{\text{eff}} \mu_B B S_z$ where S_z is the spin component along the field direction and g_{eff} is the direction dependent effective g factor [21]. Because of the relatively small spin-orbit interaction in OS, $g \approx 2$ and the anisotropy is relatively small, of the order of $\sim 10^{-3}$. Given a spin pair (e.g., PP or TT), for which the anisotropy axes of the two spins within the pair are not parallel, which is placed in a magnetic field in an arbitrary direction, then g_{eff} for one of the constituent spins is not equal to the second g_{eff} providing thus a spin mixing mechanism which is essentially a “direction sensitive” Δg mechanism. In fact, in photosynthetic reactions, the magnetic field orientation dependence of the triplet quantum yield was attributed [22] to the anisotropy of the g matrix.

In this work we report on several magnetoresponse quantities, namely MEL and magnetoconductance (MC) of devices made of homopolymer organic semiconductors in magnetic fields in the range up to 8 T, with a resolution of 10^{-4} T at low fields in the temperature range 30–280 K. We find that MC and MEL can be explained by the HF and g -anisotropy spin mixing mechanisms within a PP. We also determine the PP internal spin structure and show that it is different for OLEDs made of different organic layers; this may have implications on their electrical mobility and overall EL efficiency.

II. EXPERIMENTAL DETAILS

A solvent-cast layer (~ 150 -nm thick) of the organic semiconductor was sandwiched between a cathode made of ~ 30 -nm Ca covered by ~ 100 -nm Al and ~ 40 -nm Au films on top of a transparent anode (made of a film of indium tin oxide,

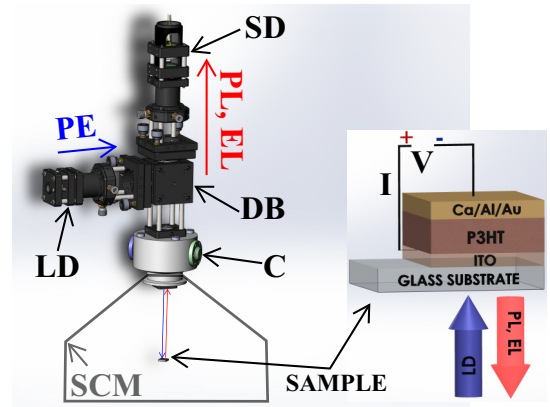


FIG. 1. Apparatus schematics. Photoexcitation (PE) beam originated at the laser diode (LD) is directed through a dichroic beam splitter (DB) onto the sample inside a superconducting magnet (SCM) placed in a cryostat. The sample is a device in which the organic semiconductor (e.g., rrP3HT, SY-PPV) is sandwiched between a transparent anode (indium tin oxide, ITO) and a cathode made of a film of Ca covered by Al and Au layers. Input light excitation and output PL and EL are directed through the glass substrate and transparent anode. For MEL and MC, the device is in the dark under forward bias, $V > 0$; EL(B) and I(B) are measured. For MPL and MPC, the device is illuminated under zero bias, $V = 0$; PL(B) and PC(B) are measured.

ITO, on a glass substrate) through which the emitted light is collected. Importantly, we did not use a hole transporting layer (e.g., PEDOT:PSS) in order not to disturb the device magnetic field response [23]. We used as active layers the light emitting polymers rrP3HT (Rieke, # 4002-EE) and Super Yellow (SY-PPV) copolymer, which is a derivative of poly(phenylenevinylene) (PPV) (MERCK, # PDY-132). The general setup structure is shown in Fig. 1.

We have measured the effect of magnetic fields on EL and current (I) under applied forward bias (5 V@8 mA for rrP3HT and 8 V@0.5 mA for SY-PPV at room temperature, provided by Keithley 2614B source meter) in the dark. The magnetoresponses, MEL and MC, are defined by $\text{MEL}(B) = [\text{EL}(B)/\text{EL}(0) - 1]$ and $\text{MC}(B) = [I(B)/I(0) - 1]$, respectively. The MEL and MC measurements were performed under fixed bias conditions; the bias was above the threshold for EL with approximately the same current at $B = 0$ for all temperatures. The devices were placed in a magnetic field B inside a variable temperature cryostat. The magnetic field was provided by a superconducting magnet with B up to 8 T. The studied device was immersed in helium vapors and the temperature was controlled by the helium flow and a heater, using a magnetic field insensitive thermometer (Lake shore, Cernox 1050, error of only 0.004% at 300 K @ $B = 8$ T). It is worth noticing that since the studied OS show an appreciable temperature dependence of both the injected current or EL it is very important to control the measurement temperature in order to minimize spurious magnetic field responses.

III. EXPERIMENTAL RESULTS

The general setup of the measuring system is shown in Fig. 1, where the current I and electroluminescence EL

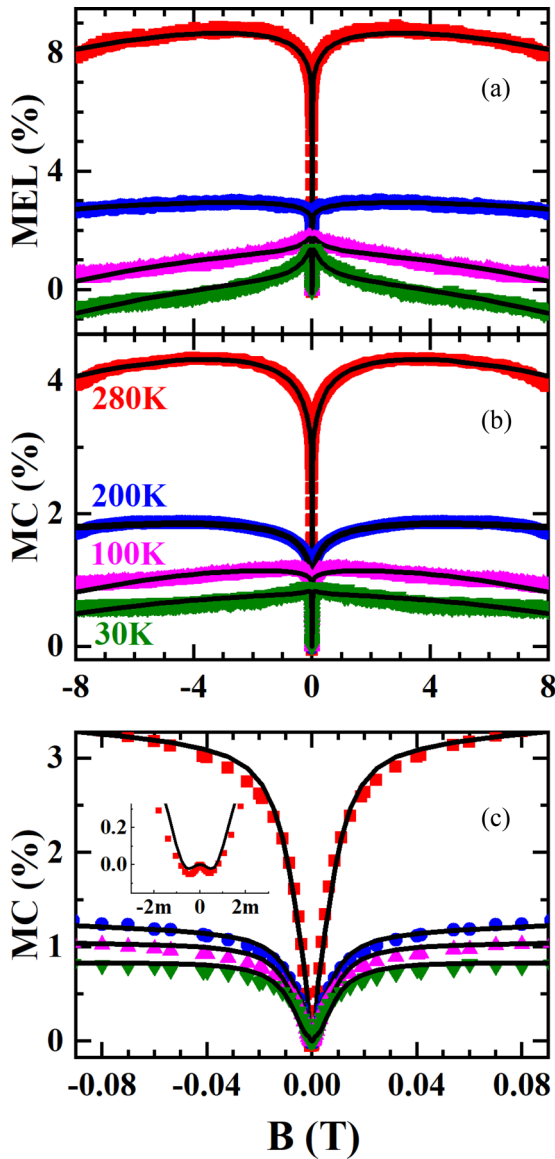


FIG. 2. The response $MEL(B)$, $MC(B)$ for SY-PPV OLED at $T = 30, 100, 200, 280$ K in the range up to $B = 8$ T. (a) $MEL(B)$ and (b) $MC(B)$ up to $B = 8$ T. (c) Enlarged low field view of $MC(B)$ for $B = 80$ mT. The inset shows high resolution data at very low fields (2 mT). Dots are experimental data, solid lines are fits to the model described in the text.

are measured as a function of B . Figures 2 and 3 show the measured $MEL(B)$ and $MC(B)$ responses for OLEDs based on SY-PPV and rrP3HT, respectively, up to $B = 8$ T at several temperatures in the range $T = 30$ – 280 K. SY-PPV is a good emitter showing relatively strong EL thus enabling MEL measurements, whereas in rrP3HT MEL could not be reliably measured with our high field experimental setup. The $MEL(B)$ and $MC(B)$ [red squares, Figs. 2(a) and 2(b), respectively] responses in SY-PPV at $T = 280$ K were found to be identical, up to a field independent constant factor; at lower temperatures the responses are less similar. We show below that a combination of HF interaction, g -factor anisotropy spin mixing mechanisms, and thermal spin polarization accounts very well for MC and MEL of both OLEDs.

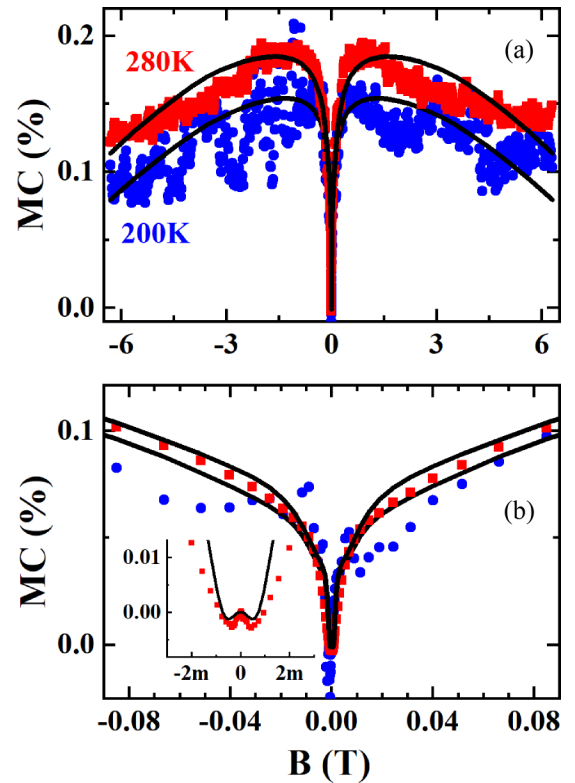


FIG. 3. The $MC(B)$ response for P3HT OLEDs at $T = 200, 280$ K in the range up to $B = 6$ T (a) and high resolution up to 80 mT (b). The inset shows high resolution data at very low fields (2 mT).

The sharp $MC(B)$ feature (full width half maximum, FWHM, of ~ 10 mT) together with the modulated structure at ultralow field (~ 1 mT) observed near $B = 0$ in Figs. 2(c) and 3(b) is the typical HF mediated response due to spin-mixing by the proton-polaron HF interaction, which for P3HT and SY-PPV is of the order of $a_{HF} \sim 0.5 \mu\text{eV}$ (HF field, $B_{HF} \equiv a_{HF}/\mu_B \sim 8$ – 9 mT) [3]. At higher fields the response due to the HF interaction saturates, so that other spin-mixing interactions that are operative at higher fields become dominant. The HF contribution to MC and MEL in organic devices in the low field regime has been accounted for and discussed in detail in various studies [3,4,24]; here we focus our attention mainly on fields where the effect of the HF interaction is already saturated.

Below we interpret the results by spin mixing due to several mechanisms. At low fields we consider the HF interaction mechanism for both MC and MEL. We attribute the intermediate field behavior to the effect of the anisotropy of the g matrix while at higher fields the effect of thermal spin polarization (TSP) becomes non-negligible [13,14] in both P3HT and SY-PPV.

IV. DISCUSSION

A. Effect of g -factor anisotropy

The g -factor anisotropy mechanism [22] is closely related to the Δg mechanism discussed previously [6,12,13]. When the g factor is anisotropic, as is usually the case for OS [17], the Zeeman energy of a pair of spins, S_1 and S_2 , can be written

as

$$H_Z = g_1(\vec{n}_1)\mu_B B S_{1z} + g_2(\vec{n}_2)\mu_B B S_{2z}, \quad (1)$$

where $\vec{n}_i = (n_{ix}, n_{iy}, n_{iz})$ are the direction cosines of the principal g -matrix z' axis with respect to the $B||z$ direction and $g_i(\vec{n}_i)$ ($i = 1, 2$) are the direction dependent effective g factor for each spin, given by [21]

$$g_i(\vec{n}_i) = [n_{ix}^2 g_{ix}^2 + n_{iy}^2 g_{iy}^2 + n_{iz}^2 g_{iz}^2]^{1/2}, \quad (2)$$

where g_x, g_y, g_z (~ 2 for OS) are the three components along the g -matrix principal axes. We note that (a) For an isotropic g matrix with $g_1 \neq g_2$, $H_Z = \mu_B B (g_1 S_{1z} + g_2 S_{2z})$, states with zero spin component $S_z = S_{1z} + S_{2z} = 0$ (e.g., singlet S and triplet T_0 in the case of PP) mix, while at high fields their energy spacing varies in proportion to B , $\Delta E_{S_z=0} \propto \mu_B |g_2 - g_1| B$ (“ Δg mechanism”, $\Delta g = g_2 - g_1 \neq 0$) [12]. (b) For anisotropic, identical but not parallel g matrices, states with zero spin mix giving an effect which is essentially an “angle dependent Δg mechanism”. For example, in the simple case, $\vec{n}_1||z$; $\vec{n}_2||x$ we obtain $H_Z = \mu_B B (g_z S_{1z} + g_x S_{2z})$; i.e., it is analogous to the Δg mechanism, $\Delta g = g_z - g_x \neq 0$, as in case (a) above.

The total Hamiltonian of the pair of spins should include, besides the Zeeman term [Eq. (1)], also the HF term [3,4] between the electronic spin S_i and neighboring nuclear spins (e.g., protons or ^{13}C), exchange, and SO coupling [1,21]. In order to quantitatively account for the effect of g -factor anisotropy on the high field MFE(B) in the studied OLEDs, we consider here only the Zeeman, hyperfine, and exchange interaction terms in the spin Hamiltonian. Consequently, the pair spin Hamiltonian in magnetic fields B is

$$H_0 = H_Z - J(\vec{S}_1 \cdot \vec{S}_2 + 1/4) + \sum_m a_{\text{HF}} \vec{I}_m \cdot \vec{S}_m, \quad (3)$$

where $m = 1, 2$, H_Z is given by Eq. (1), $J \leq 1 \mu\text{eV}$ is the exchange interaction coefficient, and a_{HF} represents the HF interaction strength with a nearby nuclei (for simplicity, we take into account only the isotropic exchange interaction and hyperfine coupling with a single proton for each polaron). For $B \neq 0$ the states are Zeeman separated into M (e.g., $M = 16$ for PP including HF with two protons, $I = 1/2$) direction-sensitive levels, having energies E_n ($n = 1, \dots, M$). The wave functions of specific spin configuration mix, thereby the spin character of each mixed state becomes B dependent. In order to calculate MFE we have to take into account the loss of coherence by spin dependent decay; we write the decay operator as

$$\Gamma = \sum_{\lambda} \gamma_{\lambda} P^{\lambda}, \quad (4)$$

where λ is the spin configuration (e.g., S or T), γ_{λ} is the spin dependent decay rate, and P^{λ} is the projection operator for the λ spin configuration. We use the stochastic Liouville equation to describe the time dependent density matrix, $\rho(t)$, which gives the coherent mixing and eventual decay of spin density,

$$\frac{d\rho}{dt} = -\frac{i}{\hbar} [H_0, \rho] - \frac{1}{2} \{\Gamma, \rho\}. \quad (5)$$

A formal solution of Eq. (5) is given by $\rho(t) = e^{-iHt/\hbar} \rho_0 e^{iH^\dagger t/\hbar}$ where $H = H_0 - i\hbar\Gamma/2$ is non-Hermitic

with $\rho_0 = \rho(t=0)$. ρ_0 is determined by the actual experiment; e.g., for spin insensitive charge injection $\rho_0 = \frac{1}{4} \sum_{\lambda} P^{\lambda}$. The density of spin configuration λ is then given by $\rho_{\lambda}(t) = \text{tr}[P^{\lambda} \rho(t)]$, yielding a decaying oscillatory behavior. Since the trace does not depend on the basis chosen we may calculate $\rho_{\lambda}(t)$ in a basis of our choice; this makes $\rho_{\lambda}(t)$ suitable for direct calculations. When a measurable quantity Y ($Y = \text{EL, PL, PC or I}$) is generated from ρ_{λ} with a spin dependent rate R_{λ} , then the total density generated rate is $dY/dt = \sum_{\lambda} R_{\lambda} \rho_{\lambda}(t)$. In steady state the total yield is

$$Y(B) = \int_0^{\infty} \frac{dY}{dt} dt = \sum_{\lambda} R_{\lambda} \int_0^{\infty} \rho_{\lambda}(t) dt. \quad (6)$$

The magnetoresponse, MY, is then obtained using the definition: $\text{MY}(B) = [Y(B)/Y(0) - 1]$. It is important to note that finite magnetoresponse, $\text{MY}(B) \neq 0$, is obtained *only* when the rates R_{λ} , and/or γ_{λ} , are spin dependent.

In a disordered sample the measured magnetoeffects are essentially a directional average over all possible angles of B with the two independent spins. Thus, to obtain MC we have to average over the solid angles Ω_1, Ω_2 of the pair of spins:

$$\text{MC}_{\text{ave}}(B) = \iint f(\Omega_1, \Omega_2) \text{MC}(\Omega_1, \Omega_2, B) d\Omega_1 d\Omega_2, \quad (7)$$

where $\text{MC}(\Omega_1, \Omega_2, B)$ is the $\text{MC}(B)$ response calculated, using Eq. (6), for a given set (Ω_1, Ω_2) . In Eq. (7) $d\Omega = \sin\theta d\theta d\varphi$, $f(\Omega_1, \Omega_2)$ is the two-angle normalized distribution function for the system, $\iint f(\Omega_1, \Omega_2) d\Omega_1 d\Omega_2 = 1$ (for isotropic disorder $f = 16^{-1} \pi^{-2}$). For the actual fitting of the data, we first determine the range of the Euler angles $\varepsilon = (\alpha, \beta, \gamma)$ of the g matrix of spin number 2 (S_2) relative to spin number 1 (S_1), while averaging with respect to the direction of B . By using a Gaussian distribution function of width σ around a certain set of angles $\varepsilon = \varepsilon_0$, we can more easily determine the preferred orientation of S_2 relative to S_1 in the amorphous organic layer.

The range of fields in which the magnetoresponse $\text{MY}(B)$ and its shape vary are controlled by the exchange J , the g anisotropy δg and spin dependent decay rate γ_{α} . It is found that in the absence of the HF and thermal spin polarization mechanisms, $\text{MY}(B)$ has a Lorentzian-like shape with FWHM that is inversely proportional to δg : $\Delta B = 2(\mu_B \delta g)^{-1} [(\hbar/\tau_d)^2 + J^2]^{1/2}$, where δg is a measure for the actual anisotropy, obtained by averaging over all directions. Note that for $\hbar/\tau_d \gg J$ FWHM is $\Delta B \approx 2\hbar/(\mu_B \delta g \tau_d)$ whereas for $\hbar/\tau_d \ll J$ it is $\Delta B \approx 2J/(\mu_B \delta g)$.

B. Magnetic field dependence: Hyperfine, g -factor anisotropy, and thermal mechanisms

We first note that at 280 K $\text{MC}(B)$ and $\text{MEL}(B)$ in SY-PPV OLED, are identical up to a field independent constant [red squares, Figs. 2(a) and 2(b)]. This points out to a common mechanism and identical species for the two magnetoeffects. Since EL is the result of e - h recombination, we analyze the measured MC and MEL as due to pairs of positive and negative polarons, PP. For PP we consider the following spin mixing interactions: (a) The HF interaction between the PP spin and the protons surrounding it [3,4], (b) The g -anisotropy mechanism discussed in detail in the preceding section,

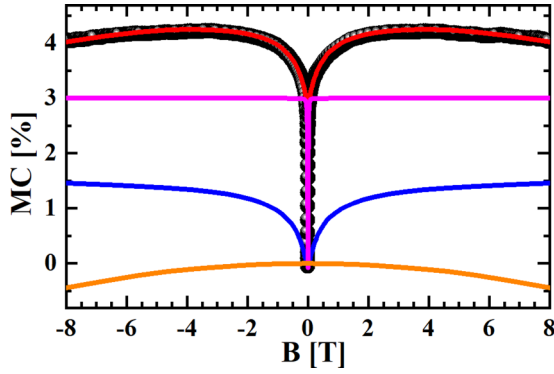


FIG. 4. Individual HF, g anisotropy and thermal polarization components for $MC(B)$ fit in SY-PPV at 280 K. Black dots: experimental $MC(B)$; red line: fit curve; magenta line: HF contribution; blue line: g -anisotropy contribution; orange line: thermal spin polarization contribution.

(c) Thermal spin polarization [13]. Following the procedure outlined above, we calculate the yield and the magnetoeffects using spin independent initial state for electrode charge injection (MC and MEL). The magnetic response $MY(B)$ is then calculated using Eq. (6) and (7), while averaging over all directions.

At $T = 280$ K and for $B < 1$ T, the difference in thermal population between the lowest Zeeman split level and the higher levels is such that MFE would be smaller than approximately 0.1%. We then do not expect that MFE due to thermal spin polarization [13] will be detectable at such low fields, but it may, however, be detectable at higher fields. We, therefore, treat the MFE due to thermal polarization similarly to the procedure outlined in our earlier work [13]. In Fig. 4 we show a demonstration for a calculated fit to

$MC(B)$ of SY-PPV, where we show separately the contributions of the HF, anisotropic g -tensor (averaged over all directions) mechanisms and the contribution of thermal polarization. As is clearly seen, the HF mechanisms gives rise to a positive contribution [$MC(B) > 0$] but is limited to very low fields ($B < 20$ mT), the g -anisotropy mechanism is also positive [$MC(B) > 0$] and is effective at intermediate fields ($0.01 < B < 1.5$ T), while thermal polarization gives rise to a relatively small negative contribution [$MC(B) < 0$] at higher fields, $B > 2$ T. It is not possible to obtain a reasonable fit at $T = 280$ K in the range $0.01 < B < 1.5$ T without taking into account the g -anisotropy mechanism.

The solid black lines in Figs. 2 and 3 are the actual fits obtained, at the temperatures indicated, for MC and MEL in SY-PPV and MC in rrP3HT OLEDs, respectively; the parameters for these fits are summarized in Table I. Importantly, the results at $T = 280$ K show that (a) For SY-PPV the two g matrices have similar g components (within 10^{-5}) in two directions (e.g., g_x, g_y) that differ substantially (by $\sim 4 \times 10^{-3}$) from g_z ; the relative angular distribution of the two g matrices is $\varepsilon_0 = (\alpha, \beta, \gamma) = (0, 0, 0)$, $\sigma = 40^\circ$. (b) For P3HT, the g -matrix components along all directions differ substantially; the angular distribution of the two polaron g matrices is $\varepsilon_0 = (\alpha, \beta, \gamma) = (0, 90^\circ, 0)$, $\sigma = 10^\circ$ (see Sec. IV A for the definition of the angular distribution). Thus, the analysis of $MC(B)$ using the g -anisotropy mechanism shows that the relative orientation of the two polarons within the PP is material dependent. The relative orientation of the two polarons that are residing on different molecules and possibly on different grains influences the mobility [25] and EL efficiency rationalizing why SY-PPV is a better OLED device. We emphasize here that the components of the g matrix were determined by fitting the $T = 280$ K response at fields below $B = 2$ T. At lower temperatures the response is less sensitive

TABLE I. Fit parameters for MC, MEL in SY-PPV and P3HT. The temperature dependent spin lattice relaxation rates $\gamma_{SL} = \tau_{SL}^{-1}$ used for the fitting are given in column 2. These values were measured [8] for P3HT and used here also for SY-PPV. In column 3 MFE stands for either MC or MEL. The subscripts S and P designate SY-PPV and P3HT, respectively. The ratios of triplet to singlet decay and dissociation rates, $\gamma_{T\pm}/\gamma_S$, $k_{T\pm}/k_S$, are given in columns 4,5,6. The g -factor anisotropy $\Delta g_y = g_y - g_x$, $\Delta g_z = g_z - g_x$ are given in column 7 and their Gaussian angle distribution, $\varepsilon = (\alpha, \beta, \gamma)$, σ in column 8. The parameters in columns 7 and 8 were determined from the $T = 280$ K response (see Sec. IV B). The letters S and P designate SY-PPV and P3HT, respectively. α, β, γ are the Euler angles (in degrees) of spin 2 relative to spin 1, and σ is the width (in degrees) of the distribution. The exchange [Eq. (3)] and hyperfine interaction [Eq. (3)] strengths are $J = 17, 16$ neV, $a_{HF} = 750, 870$ neV for SY-PPV and P3HT, respectively. The decay rate is $\gamma \approx 1 \mu s^{-1}$ and the ratio $\gamma_{T0}/\gamma_S = 1.1$ for both OLEDs.

| 1 | 2 | 3 | 4 | 5 | 6 | 7 | 8 |
|-------|----------------------------|------------------|--------------------------|----------------|--------------|--|-----------------------------------|
| T (K) | $\gamma_{SL} (\mu s^{-1})$ | MFE | $\gamma_{T\pm}/\gamma_S$ | $k_{T\pm}/k_S$ | k_{T0}/k_S | $10^3 \Delta g_y$ $10^3 \Delta g_z$ | $(\alpha, \beta, \gamma); \sigma$ |
| 280 | 12 | MC _S | 1.8 | 10 | 5 | 0.01 | S: (0,0,0); 40 |
| | | MEL _S | 1.8 | 10 | 5 | 4 | |
| | | MC _P | 1.5 | 1.3 | 1.6 | 1 | P: (0,90,0); 10 |
| 200 | 4 | MC _S | 1.7 | 3.4 | 2.8 | | |
| | | MEL _S | 1.9 | 2.1 | 2.1 | | |
| | | MC _P | 1.6 | 1.3 | 1.6 | | |
| 100 | 1 | MC _S | 1.4 | 1.4 | 1.2 | | |
| | | MEL _S | 1.3 | 0.5 | 0.6 | | |
| 30 | 0.5 | MC _S | 1.9 | 1 | 1.6 | | |
| | | MEL _S | 1.6 | 0.1 | 0.7 | | |

to the anisotropy because thermal effects become increasingly important at lower fields. We expect the g -factor anisotropy to be temperature independent, therefore we assume that the g matrix is the same at all temperatures. It is also evident that in the low field range, up to ~ 20 mT, the HF interaction mechanism, of approximate strength of $\sim 0.5 \mu\text{eV}$, is responsible for the width and sub-mT modulation. The sub-mT modulation is clearly observed in MC and MEL of both OLEDs. The species decay times, together with the exchange interaction, also play a significant role at higher fields where the g -anisotropy mechanism becomes important. At yet higher fields TSP is responsible for the nonsaturated behavior.

V. SUMMARY

We have shown that in OLEDs that are constructed from homopolymer light emitting layers in which PPs are long lived, such as SY-PPV and rrP3HT, a spin mixing mechanism due to the anisotropy of the active layer g factor has a significant effect on the measured MC(B) and MEL(B) at fields on the order of ~ 1 T. This is very different from the magneto-photoconductance measured for organic photovoltaic cells made of donor-acceptor blends, where the effect due to the different donor-acceptor g factors is significant at much higher fields (> 8 T). The different range of fields in which the

MFE is significant arises from the different decay times of PP in homopolymers ($\sim 1 \mu\text{s}$) and charge transfer excitons in the blend (< 1 ns); the longer the decay time the smaller the field range. We also found that the internal structure of the long-lived PP is material dependent; this is important for the overall electrical mobility of organic semiconductors. It has been observed that in polycrystalline P3HT the mobility is larger for a morphology in which the relative orientation of neighboring molecules is face to face [25,26]. Thus, our finding that in SY-PPV the relative orientation of polarons in a PP (in which each polaron resides on a different molecule) is different than in P3HT, is in line with the fact that SY-PPV has a different EL efficiency. In addition, the g -anisotropy mechanism in OLEDs made of homopolymers may substantially manipulate MEL by fringe fields created by patterned magnetic domains [27].

ACKNOWLEDGMENTS

This work was supported by the Israel Science Foundation (ISF, Grants No. 598/14; E.E., No. 914/15; E.L., No. 488/16; N.T.), by the Israel Science Foundation Bikura Program (No. 1508/14; E.L.), and by Volkswagen Stiftung (No. 88116; E.L.).

-
- [1] R. E. Merrifield, Magnetic effects on triplet exciton interactions, *Pure Appl. Chem.* **27**, 481 (1971).
- [2] P. A. Bobbert, T. D. Nguyen, F. W. A. van-Oost, B. Koopmans, and M. Wohlgenannt, Bipolaron Mechanism for Organic Magnetoresistance, *Phys. Rev. Lett.* **99**, 216801 (2007).
- [3] T. D. Nguyen, G. Hukic-Markosian, F. J. Wang, L. Wojcik, X. G. Li, E. Ehrenfreund, and Z. V. Vardeny, Isotope effect in spin response of π -conjugated polymer films and devices, *Nat. Mater.* **9**, 345 (2010).
- [4] T. D. Nguyen, B. R. Gautam, E. Ehrenfreund, and Z. V. Vardeny, Magnetoconductance Response in Unipolar and Bipolar Organic Diodes at Ultrasmall Fields, *Phys. Rev. Lett.* **105**, 166804 (2010).
- [5] C. R. Timmel, U. Till, B. Brocklehurst, K. A. McLauchlan, and P. J. Hore, Effects of weak magnetic fields on free radical recombination reactions, *Mol. Phys.* **95**, 71 (1998).
- [6] A. J. Schellekens, W. Wagemans, S. P. Kersten, P. A. Bobbert, and B. Koopmans, Microscopic modeling of magnetic-field effects on charge transport in organic semiconductors, *Phys. Rev. B* **84**, 075204 (2011).
- [7] J. J. Burdett and C. J. Bardeen, Quantum beats in crystalline tetracene delayed fluorescence due to triplet pair coherences produced by direct singlet fission, *J. Am. Chem. Soc.* **134**, 8597 (2012).
- [8] V. I. Krinichnyi, P. A. Troshin, and N. N. Denisov, Structural effect of fullerene derivative on polaron relaxation and charge transfer in poly(3-hexylthiophene)/fullerene composite, *Acta Mater.* **56**, 3982 (2008).
- [9] J. Rybicki, T. D. Nguyen, Y. Sheng, and M. Wohlgenannt, Spin-orbit coupling and spin relaxation rate in singly charged π -conjugated polymer chains, *Synthetic Met* **160**, 280 (2010).
- [10] B. R. Gautam, T. D. Nguyen, E. Ehrenfreund, and Z. V. Vardeny, Magnetic field effect on excited-state spectroscopies of π -conjugated polymer films, *Phys. Rev. B* **85**, 205207 (2012).
- [11] S. Zhang, N. J. Rolfe, P. Desai, P. Shakya, A. J. Drew, T. Kreouzis, and W. P. Gillin, Modeling of positive and negative organic magnetoresistance in organic light-emitting diodes, *Phys. Rev. B* **86**, 075206 (2012).
- [12] A. H. Devir-Wolfman, B. Khachatryan, B. R. Gautam, L. Tzabary, A. Keren, N. Tessler, Z. V. Vardeny, and E. Ehrenfreund, Short lived charge transfer excitons in organic photovoltaic cells studied by high field magnetophotocurrent, *Nat Commun* **5**, 4529 (2014).
- [13] B. Khachatryan, A. H. Devir-Wolfman, L. Tzabari, N. Tessler, Z. V. Vardeny, and E. Ehrenfreund, Magneto-Photocurrent in Organic Bulk Hetero-Junction Photo-Voltaic Cells at Low Temperatures and High Magnetic Fields, *Phys. Rev. Appl.* **5**, 044001 (2016).
- [14] J. Wang, A. D. Chepelianskii, F. Gao, and N. C. Greenham, Control of exciton spin statistics through spin polarization in organic optoelectronic devices, *Nat. Commun.* **3**, 1191 (2012).
- [15] S. L. Bayliss, N. C. Greenham, R. H. Friend, H. Bouchiat, and A. D. Chepelianskii, Spin dependent recombination probed through the dielectric polarizability, *Nat. Commun.* **6**, 8534 (2015).
- [16] M. Kavand, D. Baird, K. v. Schooten, H. Malissa, J. M. Lupton, and C. Boehme, Discrimination between spin-dependent charge transport and spin-dependent recombination in π -conjugated polymers by correlated current and electroluminescence-detected magnetic resonance, *Phys. Rev. B*, **94**, 075209 (2016).

- [17] A. Sperlich, H. Kraus, C. Deibel, H. Blok, J. Schmidt, and V. Dyakonov, Reversible and irreversible interactions of poly(3-hexylthiophene) with oxygen studied by spin-sensitive methods, *J. Phys. Chem. B* **115**, 13513 (2011).
- [18] J. D. Ceuster, E. Goovaerts, A. Bouwen, J. C. Hummelen, and V. Dyakonov, High-frequency (95 GHz) electron paramagnetic resonance study of the photoinduced charge transfer in conjugated polymer-fullerene composites, *Phys. Rev. B*, **64**, 195206 (2001).
- [19] H. Malissa, R. Miller, D. L. Baird, S. Jamali, G. Joshi, M. Bursch, S. Grimme, J. v. Tol, J. M. Lupton, and C. Boehme, Revealing weak spin-orbit coupling effects on charge carriers in a π -conjugated polymer, *Phys. Rev. B* **97**, 161201 (2018).
- [20] G. Joshi, M. Y. Teferi, R. Miller, S. Jamali, M. Groesbeck, J. v. Tol, R. McLaughlin, Z. V. Vardeny, J. M. Lupton, H. Malissa, and C. Boehme, High-Field Magnetoresistance of Organic Semiconductors, *Phys. Rev. Appl.* **10**, 024008 (2018).
- [21] A. Abragam and B. Bleaney, *Electron Paramagnetic Resonance of Transition Ions* (Oxford University Press, London, UK, 1970).
- [22] S. G. Boxer, C. E. D. Chidsey, and M. G. Roelofs, Anisotropic magnetic interactions in the primary radical ion-pair of photosynthetic reaction centers, *Proc. Nat. Acad. Sci. USA* **79**, 4632 (1982).
- [23] T. D. Nguyen, Y. Sheng, J. Rybicki, G. Veeraraghavan, and M. Wohlgenannt, Magnetoresistance in π -conjugated organic sandwich devices with varying hyperfine and spin-orbit coupling strengths, and varying dopant concentrations, *J. Mater. Chem.* **17**, 1995 (2007).
- [24] V. Prigodin, J. Bergeson, D. Lincoln, and A. J. Epstein, Anomalous room temperature magnetoresistance in organic semiconductors, *Synth. Met* **156**, 757 (2006).
- [25] R. J. Kline, M. D. McGehee, and M. F. Toney, Highly oriented crystals at the buried interface in polythiophene thin-film transistors, *Nat. Mater.* **5**, 222 (2006).
- [26] H. N. Tsao and K. Mullen, Improving polymer transistor performance via morphology control, *Chem. Soc. Rev.* **39**, 2372 (2010).
- [27] N. J. Harmon, M. Wohlgenannt, and M. E. Flatté, Manipulation of the electroluminescence of organic light-emitting diodes via fringe fields from patterned magnetic domains, *Appl. Phys. Lett.* **109**, 243303 (2016).